CYBERNETICS

The modern definition of cybernetics arose in the study of machines containing feedback and computing subsystems. The second world war and available technology combined to give a generation of more "intelligent" machines than previously utilized. One of the more important persons in this endeavor was Norbert Wiener, mathematician, electrical engineer, and professor at Massachusetts Institute of Technology. He had been at MIT since 1920 and was involved in deriving several feedback and communications filtering theories, some of which were classified in the second world war but all subsequently published. Wiener's important theories on nonlinear systems were developed shortly after the second world war. As a result of Professor Wiener's broad and incisive knowledge in many areas of science and engineering beyond mathe-

matics, he proposed a new word, *cybernetics,* in 1947, to describe a scientific frontier: a parallel and interacting study of intelligent machines and living organisms (1,2). The objectives of such parallel study are to increase understanding of living organisms by mathematically modeling their many systems and subsystems, with an important engineering goal, in many cases, of improved design of machines. An obvious example is the pilot-aircraft feedback control problem. In more recent studies both parallel and interacting, one may build electromechanical models of aspects of motor physiology, which can then be incorporated in robots, and further apply known sensory response characteristics found in perception and physiology studies to make the robot more adaptive and thus more intelligent. Computational models of the central nervous system can then be used to further this design paradigm in robotics, another branch of cybernetics.

The original definition of cybernetics is still that found in many languages today and it also applies to organized groups of living organisms, such as societies with their political, social, and economic subsystems and their interactions. Computational modeling is also applied to these problems to find dynamic properties that might be utilized in predictions, and in several fields this endeavor is nominally cybernetics. It is possibly this aspect of cybernetics that is related in its etymology most closely to the Greek root *Kuber,* which is also the root word for government. In a sense, cybernetics was intended also to put government on a scientific and rational basis, and an extensive series of meetings of the "Cybernetics Group" from 1946 to 1953 brought forth consideration of these diverse aspects of cybernetics, including especially the social aspects (3).

However, the cybernetics of greatest interest to electrical and electronic engineers is the parallel study of nonlinear feedback and nonlinear signal processing circuits and systems to model the peripheral and central nervous systems of living organisms. Thus, cybernetics can be "modeling the brain" in a very imprecise definition, but still related etymologically to the other, closer Greek root word, *Kubernetes,* a steersman or navigator. The earliest meeting of the minds on this subject extended to 1935, and one of the well-known later results was the "Pitts-McCulloch Neuron," the ancestor of much of modern work in the field of neural networks, another descendent field of cybernetics.

In some areas of physiology and biophysics the quantitative analysis and modeling of living processes was indeed already on the level that Wiener and colleagues envisioned. The cybernetics meetings included some of these pioneering physiologists, biophysicists, and psychologists. No aspect of cybernetics arose in a vacuum, but the emergent viewpoint was different. It was and is the parallel study of machines and living organisms, a liberal view that includes but is not restricted to precise modeling, data analysis, and design. Further, the assumptions of modeling living organisms must be grounded in some known aspects of the physiology or biophysics. Thus there are overlapping areas of cybernetics with many fields: physiology, biophysics, computer science, robotics, artificial neural networks, and vision science to name a few. Cybernetics simply follows the scientific method, where the theorists and the experimentalists are not necessarily the same people. Cybernetic models are actually hypotheses, and they flow into experimental science as well as to engineering design. It is never immediately clear how good these models are from a scientific or engineering standpoint, and thus cybernetics is a continuously growing field.

Historically the field of cybernetics grew at MIT, where since 1935 seminars of physiologists, biophysicists, neurologists, electrical engineers, physicists, mathematicians, and psychologists took place continually. This intellectual effort spread to other institutions, such as the California Institute of Technology, the University of California Los Angeles, the Max Planck Institute for Biological Cybernetics in Tubingen, Germany, the University of Southern California, the University of California San Diego, Cambridge University, Northwestern University, the Australian National University, Boston University, the University of Adelaide, the University of Pennsylvania, and Drexel University. The field of cybernetics and its biological aspects are represented in at least 20 modern archival journals and many conferences sponsored by the Institute of Electrical and Electronic Engineers (IEEE), International Neural Network Society, Biophysical Society, Optical Society of America, Biomedical Simulations Resource of the University of Southern California, and Society for Neuroscience and the Biomedical Engineering Society, among others.

BIOLOGICAL NEURONS, OR NERVE CELLS

By 1947, a fairly precise but simple picture of how nerve cells computed and signaled their outputs had been assembled. It was already clear that nerve cells did not operate as "all-or-none" except in their long-distance impulse transmission along axons. The impulse is essentially a solitary wave, propagated without loss by means of active ionic processes involving sodium, potassium, and calcium. The passive resistance-capacitance electrical properties of the membrane enclosing the nerve cell were known, and it was clear that nerve cells could, and did, compute continuous sums and differences and products. Among others, the work of Rushton, Hodgkin, Eccles, and Hartline showed this. These computations by nerve cells were quantitatively described by continuous mathematics of differential equations, so the "brain as a digital computer" could be seen then as an oversimplification. The brain is modular, so in some aspects, such as general flow of information or at gating synapses, parallels could be drawn between the brain and the digital computer, but such theory lacks the necessary thorough grounding in neurophysiology.

Passive Nerve Cell Input Computations

Because the treelike structure of the nerve cell, the dendritic tree, is often electrically passive, the number of synaptic contacts on the dendrites and their electrically continuous nature implies a number of states of the biological neuron far in excess of two. But how the immense combinatoric sums are used in actual computation is still not clear. It does not seem possible at this point to utilize these facts to demonstrate clearly how to mediate or represent functions of memory or consciousness. But, on the other hand, a model involving growth and decay, by darwinian algorithms, of hexagonal regions of cortical activity is a strong beginning to representation of thought or cognition (4). Studies on more peripheral and sensory neurophysiology have led to somewhat deeper levels of understanding, in knowing exactly how the environmental information is encoded and transmitted. This has often been

accomplished by neurophysiological studies on lower species such as insects.

FUNDAMENTAL MATHEMATICAL IDEAS FOR CYBERNETICS

Modern control system theory and communication theory in electrical engineering forms a good basis for mathematical descriptions in cybernetics. An overwhelming need in this work is the ability to include the effects of nonlinearities, of both the no-memory and the memory type. Professor Wiener's outstanding contribution to this mathematics was first reported in 1949, as means to analyze and synthesize nonlinear systems. From the viewpoint of perturbation theory, a linear approximation will usually be a satisfactory beginning for analysis around the equilibrium state. But biological systems will always possess significant nonlinearities, so nonlinear theory is essential.

The forms of mathematical descriptions are typically differential equations, or integral operators on a known input, or a mixture of both. Under a very general set of assumptions, the Volterra integral operator, or functional operator, series can be derived as a solution to a given nonlinear differential equation (5). This can be considered a polynomial inversion of the differential operators. The uniform convergence of this solution under a wide category of conditions has been proven. In general, however, useful system identification methods apply to only the kernels of the integral operators, in the orthogonalized form derived by Wiener (6,7). The nonlinear differential equation does not admit a general, direct, and useful method of identification of its parameters and functions.

NONLINEAR NERVOUS SYSTEM COMPUTATION

Nonlinear functions are common in the transduction of information in the nervous system. Threshold, saturation, compression, adaptation of gain, light and dark adaptation, automatic gain and bandwidth control, and directional sequence dependence are most evident among the many discovered. The synapse in the nervous system is substantially more complex than the simple sum or difference operator. The synapse has temporal dynamics and significant nonlinear properties and can compute products and quotients. For example, the two variables at a point of connection of a synapse to a postsynaptic nerve membrane, the postsynaptic conductance and the postsynaptic voltage, are multiplied by the Ohm's law property of nerve membranes to produce a product of presynaptic activity and existing postsynaptic activity. In many cases this becomes dominated by the linear sum, which is a function of the ionic species of the conductance. In others, where the equilibrium potential of the ion is close to the existing membrane potential, the multiplication dominates. The latter is often called "shunting inhibition." In principle, any change of conductance may include a shunting component.

The possibility of a distribution of multipliers in the nervous system fits well with the theorem, proven by M. Schetzen (7), that any Volterra operator can be synthesized to a specific accuracy by a finite number of multipliers and linear systems. This provides a close mathematical link to the nervous system. In many physiological studies there is a need to know whether nerve cell connections are positive (excitatory) or negative (inhibitory), or feedback or feedforward. For example, the visual systems of many living organisms are capable of good velocity estimation, and to know how this is accomplished requires knowledge of the polarities and points of connection of synapses. Only a limited analysis of this problem is possible using neuroanatomical methods. However, given a sufficiently complex nonlinear theory, such as the Volterra series, capable of being reduced to multipliers and linear blocks, a parallel, cybernetic array of computational and physiological experiments may give some aid to understanding how the nervous system accomplishes the computations it is making. First one constructs such a model, subjects it to computation, and then alters the model to improve the fit to the data. In the course of this synthesis by iterated analysis, further experimental tests may be suggested.

Volterra and Wiener Series

One of the most important cybernetic developments by Wiener was to bring mathematics of systems analysis to a more usable form to both identify and characterize the nonlinear system. Applications of this work have been extensive in electrical and electronic engineering (6–10). First, the Volterra series is a generalization of linear convolution to multiple convolution integrals, over instants of time and space that encompass the integral-functional nature of system nonlinearities. The conditions for convergence are not severe, consisting alone of systems without infinite memory or output step discontinuities. Wiener took the Volterra series and orthogonalized it and further derived a set of functions to express the kernels. The time-dependent behavior of the kernels of the integrals is expressed by Laguerre function impulse responses, with Hermite polynomials and multipliers to combine the Laguerre functions into the kernels themselves. Gaussian distributed white-noise input to the system is needed to define, or find, the parameters by expectation operations. The most important further development was by Y. W. Lee and M. Schetzen, who showed that a nonparametrized Wiener kernel could be derived from crosscorrelating the input with the output of the system. This method, called the Lee-Schetzen algorithm, and its many variations and improvements are the bases by which most modern applications of the Volterra-Wiener theory are made (7). The sum-of-sinusoids and M-sequence methods have found considerable recent usage (8,9) in improving the signal-to-noise ratio of the kernel estimates. Because the orthogonalization of Volterra series by the Gram-Schmidt procedure yields the Wiener series, the Volterra kernels can be calculated from the Wiener kernels, and vice versa. Usually the Volterra kernels would be derived from a given known or assumed system structure, and the Wiener kernels from the input-output data by the Lee-Schetzen algorithm with other improvements. The M-sequence, for example, tends to improve the signal-to-noise ratio of the kernel estimates and shorten the required record lengths (8,9).

The Volterra-Wiener theory and method is the most general for characterizing and identifying smooth, nonoscillating nonlinear systems with finite memory. The Volterra-Wiener theory also generates a procedure for finding the inverse of a nonlinear system to any given degree. This is essentially how the differential equation is solved by assuming a Volterra series solution and applying perturbation theory (5,7,10). Further, the inverse of the nonlinear part aids the analysis and

design of nonlinear feedback systems. In general, an iterative procedure for analysis of nonlinear systems can be set up in the following way. An unknown nonlinear system can be subjected to appropriate noise inputs and the Wiener kernels identified by the crosscorrelation or other algorithm. From some minimal knowledge of the structure of the system, diagrams of linear operators and multipliers can be developed that then give the Volterra kernels, from which the corresponding Wiener kernels can be calculated. These can be compared, and modifications can be made to the assumed structures to give a better fit, in some sense. Therefore, this represents a nonlinear input–output systems analysis with identification experiments and iterative computational experiments to synthesize a system structural model.

CYBERNETICS OF A VISUAL SYSTEM

A wide-ranging study of biology, neuroanatomy, neurophysiology, and mathematics of systems is required to make a meaningful cybernetic model of only a part of an organism. Since the number of nerve cells is smaller in insects than in vertebrates, and insect behavior is perhaps more stereotyped, insect vision has received considerable study in a cybernetic manner. The Max-Planck Institute for Biological Cybernetics in Tubingen, Germany was founded on this kind of work, which always views the animal in a feedback loop with its predominating visual sensing of position, velocity, and acceleration paramount in the nervous system. Indeed, the majority of nerve cells in the brains of insects respond to visual stimuli. Of these, perhaps velocity is the most important. Some relative velocity between organism and environment is necessary for evolution, development, and learning (12). Velocity can be considered a most basic biological variable. Thus the more detailed cybernetics in the following subsection has concentrated on the insect's visual system and its transduction of the relative velocity or motion of the organism and environment.

Motion Detection System in Insects

The primary visual system of insects has a highly regular structure, dominated by a retinotopic organization. It consists of a pair of multifaceted eyes known as the *compound eyes,* two optic lobes, one on each side of the head, and the tracts and projection centers of the visual interneurons in the protocerebrum [see Strausfeld (12) for more details]. In flies, each compound eye is composed of approximately 3000 to 4000 *ommatidia* (tiny eyes). Each ommatidium is a functional unit comprising a lenslet and a retinula, containing eight receptor or retinular cells labeled R1–R8. The optic lobes convey information from the compound eyes to the brain. They each comprise three retinotopically connected visual ganglia, commonly known (from the periphery inward) as the *lamina,* the *medulla,* and the *lobula,* or *lobula complex* in some insect orders. In Diptera (true flies) the lobula complex is divided into two parts: an anterior part, the *lobula,* and a posterior part, the *lobula plate.*

The synaptic neuropils in the visual ganglia are strictly organized into columns and strata. Both the lamina and medulla are composed of structurally identical parallel synaptic compartments, or columns, that exactly match in number the ommatidia in the retina. However, the retinotopic periodicity of the lamina and medulla is coarsened by the columnar structure of the lobula: There is only one lobular column for every six medullary ones. Each column in the lamina, known as an *optic cartridge,* receives inputs from a group of six photoreceptors (R1–R6) that share the same visual axis as the overlaying ommatidium, and projects outputs to the medulla column lying directly beneath it. Each lamina cartridge houses six relay cells, the most prominent of which are the *large monopolar* cells (LMCs) L1 and L2. These two cells form the central elements in every optic cartridge. They receive the majority of the photoreceptor synapses and project retinotopically to the medulla. They are considered a major channel for relaying information about the intensity received by a single sampling station from the retina to the medulla. (For more comprehensive reviews of the anatomical structure and function of the lamina pathways, see, e.g., pp. 186–212 and 317–359 in Ref. 13 and pp. 457–522 in Ref. 14.)

The medulla has the most complex anatomical structure of any neuropil in the optic lobe and is characterized by an extensive network of lateral connections (see pp. 317–359 in Ref. 13 and pp. 428–429 in Ref.10 for a review). It contains a variety of functionally different units ranging from simple contrast detectors to directional and nondirectional motion sensitive neurons (pp. 377–390 in Ref. 10). Although little is known about the synaptic interconnections within the medulla, two major retinotopic projection modes, directly involving laminar units, have been recognized: one involved in color coding, the other in motion information processing. In the first, wide-field transmedullary neurons get inputs from a laminar cell L3 and the receptor pair R7/R8, which make no contacts in the lamina, and output to a large variety of retinotopic columnar neurons in the lobula. In contrast, the second projection mode involves small-field medullary relays: they derive their inputs from R1–R6 via the LMCs and synapse onto two bushy cells, T4 and T5, which provide inputs to wide-field color blind motion-sensitive neurons in the lobula plate. This suggests that at the level of the lamina there is already segregation of retinotopic projections to the lobula and lobula plate.

The medulla is the most peripheral structure in which movement detection takes place. However, the motion computation center in flies appears to be the *lobula plate,* the posterior part of the third visual ganglion. The lobula plate houses about 50 identifiable neurons, all of which are *directionally selective movement detecting* (DSMD) neurons and appear to form part of the optomotor control system of the insect. Most of these cells are wide-field DSMD neurons that seem to share a common network of presynaptic elements derived from the medulla. This group of DSMD neurons comprises several classes of tangential cells that respond to whole-field horizontal or vertical motion (pp. 317–359 and 391–424 in Ref. 13 and pp. 483–559 in Ref. 14). They receive both excitatory and inhibitory inputs from large retinotopic arrays of small-field *elementary movement detectors* (EMDs), which possess opposite preferred directions. Figure 1 illustrates the basic functional structure of a wide-field DSMD neuron. It is not yet known whether these small-field EMDs reside in the medulla, lobula, or lobula plate. Nonetheless, it is widely believed that they operate on the principle of a nonlinear asymmetric interaction of signals derived from adjacent cartridges of the ommatidial lattice [see, e.g., Kirschfeld (15), pp. 360–390 in Ref. 13, and pp. 523–559 in Ref. 14].

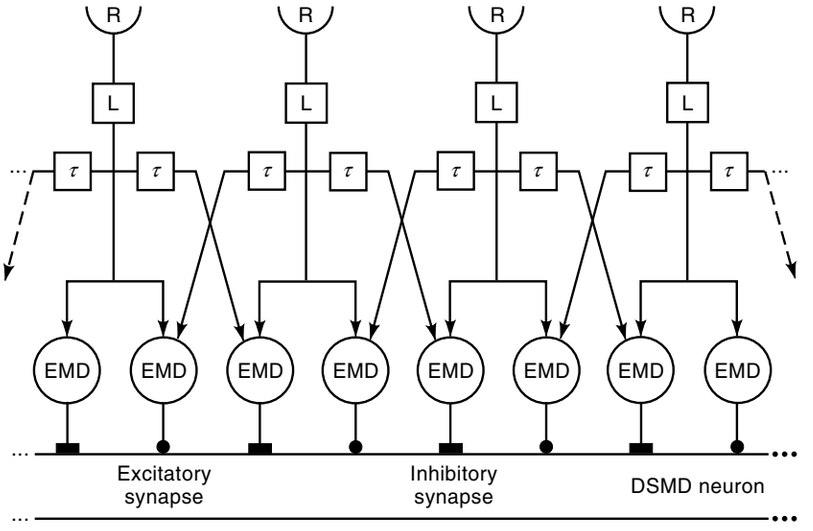

Figure 1. Schematic representation of a DSMD neuron. The DSMD neuron receives excitatory and inhibitory signals from an array of functionally identical EMDs, which differ only with respect to the orientation of their sampling bases. Each EMD receives two inputs from adjacent lamina cartridges (box L), which are fed by the receptor cells (R).

One wide-field DSMD neuron that has been extensively studied for more than two decades is the giant heterolateral H1 neuron of the fly. It responds to horizontal motion presented to the ipsilateral eye in the forward (regressive) direction, and it is inhibited by motion presented in the backward (progressive) direction. There is only one H1 neuron in each lobula plate. The main role of the H1 neuron appears to be the control of the optomotor torque response. The two bilaterally symmetric H1 cells exert mutual inhibition; thereby each cell is particularly sensitive to either clockwise or anticlockwise rotatory (yaw) motion of the visual field. The EMDs feeding the H1 neuron derive their inputs from the photoreceptors R1–R6. Franceschini and co-workers (pp. 360–390 in Ref. 13) recorded a sequence dependent response from the H1 neuron by successively stimulating the photoreceptor pair (R1, R6) within a single ommatidium. In particular, they found that the sequence R1 → R6 evoked an excitatory response whereas the sequence R6 → R1 induced an inhibitory or no response, which was in accordance with the preferred and nonpreferred directions of the H1 neuron, respectively.

Elementary Movement Detection

The EMD is the minimum prerequisite for directionally selective detection of motion in the visual field. It is based on the principle of asymmetrical interaction between two adjacent channels (Fig. 2). The visual field is sampled at two receptor regions, R_1 and R_2. The signal from one receptor is passed through an "appropriate" time delay, such as a low-pass filter of time constant τ, before interacting with the signal from the adjacent channel. The asymmetry between the two input channels is necessary for the detector to acquire direction selectivity. For if the system were symmetric, the two input channels could be interchanged without altering its response. This would be equivalent to reversing the direction of motion but still obtaining the same response. Therefore, without an asymmetrical interaction, the movement detector loses its ability to respond differentially to motion in opposite directions.

There exist mainly two general schemes for the realization of the asymmetrical interaction. One works by detecting a specific *conjunction* of excitation in the preferred direction (Fig. 2a), the other by rejecting the *null stimulus* by a *veto* operation (Fig. 2b). The best-known conjunctive scheme is the correlation model proposed by Hassenstein and Reichardt in 1956 to account for the characteristics of insect optomotor response (14). In this model, the interaction between adjacent channels is implemented by a multiplication followed by an infinite time-averaging operation (i.e., a correlation).

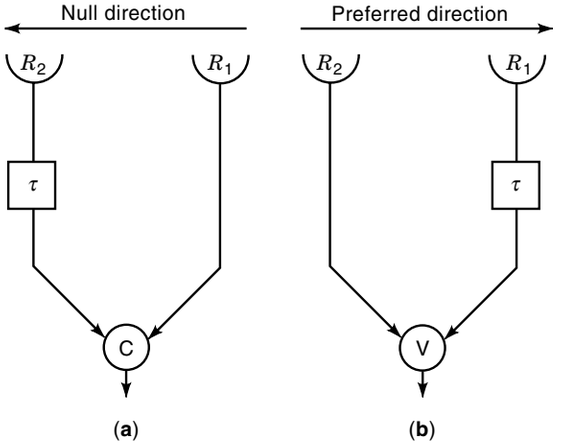

Figure 2. The elementary movement detector. (a) Conjunctive scheme: If the signals from the two adjacent channels arrive simultaneously at C (preferred direction), then a conjunction of excitation is detected signaling motion; whereas if the two signals arrive separately, the unit C remains quiescent. (b) Veto scheme: If the two signals reach V concurrently (null direction), they cancel each other and no motion is signaled. However, if the two signals arrive to V separately (preferred direction), the veto signal is unable to suppress the other signal, which indicates motion.

The first veto scheme was proposed by Barlow and Levick in 1965 (16), who discovered that inhibition is the mechanism underlying directional selectivity of ganglion cells in the rabbit retina. They suggested that inhibition is triggered selectively in such a way that at each subunit of the receptive field a delayed inhibitory mechanism vetoes the excitatory re-

sponse in the null direction, but appears too late to cancel the response in the preferred direction. Barlow and Levick demonstrated that directional selectivity of retinal ganglion cells is based on sequence discrimination within small-field synaptic subunits, or EMD. More specifically, they showed that over the whole receptive field, successive stimulation of two subunits close to each other caused a response that depends on whether the order corresponds to motion in the preferred or null direction, but the effect decreased at greater separations.

The initial stages of movement detection in insects also appear to be based on sequence discrimination by EMDs. Both behavioral and electrophysiological experiments on flies indicate that movement detection takes place between neighboring points of the sampling lattice of the eye. For example, sequential stimulation confined to pairs of identified photoreceptors in single ommatidia induced optomotor turning reactions in the fly (15) and evoked directional responses in the H1 neuron of the fly (pp. 360–390 in Ref. 13). However, the nature of the mechanism mediating direction selectivity in insects remains unresolved, despite numerous investigations attempting to unlock the mystery. Some scientists believe that it is excitatory, others suggested that it is inhibitory, yet there are others who believe that it is both (see Ref. 17 for a further discussion). It is not the aim here to resolve the conflict; however, in the next section we present a neural network architecture based on the mechanism of shunting inhibition that can account for the response of the H1 neuron.

SHUNTING INHIBITORY MOTION DETECTION

Shunting lateral inhibition is a biophysical process in which the synaptic conductance of inhibitory channels is controlled in a nonlinear manner by voltages of nearby cells or cell subunits. It can be described by a nonlinear ordinary differential equation of the form

$$\frac{de(t)}{dt} = L(t) - ae(t)\left[1 + \sum_j k_j f_j(v_j)\right] \tag{1}$$

where e represents the activity of a cell or cell subunit, interpretable as the deviation of the membrane voltage from the resting potential; $L(t) \geq 0$ is the external input to the cell; $a > 0$ is the passive decay constant; $k_j \geq 0$ represents the connection strength of the jth inhibitory synapse; v_j is the potential controlling the conductance of the jth synapse; and f_j is the activation function: it is continuous, positive, monotonic increasing for positive arguments and represents the output transfer function that converts the membrane voltage v_j to a firing rate $f(v_j)$.

The *shunting inhibitory motion detector* (SIMD) is a movement detector where the nonlinear interaction at the EMD level is mediated by shunting lateral inhibition. The response of each EMD is described by a pair of coupled ordinary differential equations:

$$\begin{aligned} \frac{dv(t)}{dt} &= L_1(t) - \frac{1}{\tau}v(t), \\ \frac{de(t)}{dt} &= L_2(t) - ae(t)[1 + kf(v)] \end{aligned} \tag{2}$$

where $e(t)$ is the EMD output, L_1 and L_2 are the external inputs of the EMD, v is the delayed inhibitory input, and τ is the time constant of the delay filter. Next, we will discuss the functional characteristics of this detector and compare them to those of fly DSMD neurons.

Characteristic Responses of SIMD

In this section we investigate both the transient and steady-state response characteristics of the SIMD and compare them to those of the fly H1 neuron. To conduct an analysis of the SIMD functional properties, an approximation of its response is in order. In general, the system of Eq. (2) is not amenable to an elementary treatment to yield an explicit solution. However, approximate solutions can be obtained if the input signals satisfy certain conditions. Perturbation methods are used to obtain approximate solutions of nonlinear differential equations. For inputs of the form

$$L_i(t) = L_0 + cl_i(t), i = 1, 2$$

where the contrast $|c| < 1$, the system of differential equations of Eq. (2) admits a unique solution that is continuous in both t and c. Therefore, $e(t)$ and $v(t)$ can be expressed as

$$\begin{aligned} v(t) &= x_0 + cx(t) \\ e(t) &= y_0 + cy_1 + c^2y_2 + \cdots = \sum_{n=0} c^n y_n \end{aligned} \tag{3}$$

Differentiating Eq. (3) and substituting for $f(v) = f(x_0 + cx)$ its Taylor series expansion into Eq. (2) yields the following equations:

$$\begin{aligned} x_0 &= \tau L_0 \\ \dot{x} &= l_1(t) - \frac{1}{\tau}x = l_1(t) - bx, \\ y_0 &= \frac{L_0}{\alpha}, \text{ where } \alpha = a[1 + kf(x_0)] \\ \dot{y}_1 &= l_2(t) - akf'(x_0)y_0x - \alpha y_1, \\ \dot{y}_n &= -ak\sum_{j=1}^{n} \frac{f^j(x_0)}{j!}x^j y_{n-j} - \alpha y_n, \text{ for } n \geq 2 \end{aligned} \tag{4}$$

The pth order approximation of the EMD response is given by

$$e_p(t) = \sum_{j=0}^{p} c^j y_j(t) \tag{5}$$

Note that the smaller is c, the more accurate is the approximation. Thus, for low-contrast stimuli one could always get a fairly good approximation to the response by solving the set of linear differential equations in Eq. (4).

Response to Drifting Gratings

Sine-wave gratings are commonly used in vision to evoke the spatial and temporal frequency responses of visual systems. Drifting gratings have been extensively used to study the response of the motion detection system in insects. Let $L(s, t)$ be a drifting sine-wave grating,

$$L(s, t) = L_0 + cL_0 \cos(2\pi f_t t + 2\pi \mu f_s s + \varphi) \tag{6}$$

where s is the spatial dimension, f_s is the spatial frequency in cycles/deg, f_t is the contrast frequency in hertz, t is time, μ is the direction of motion ($\mu = -1$ for leftward motion and $+1$ for rightward motion), and φ is the initial phase. The steady-state response of a SIMD to such drifting sine-wave grating usually oscillates around an average response that depends strongly on the direction, contrast, and spatial and temporal frequency contents of the moving pattern.

If only nonlinearities up to second order are considered, then the response of a SIMD consisting of two mirror symmetric EMDs, sharing the same inputs but having different polarities (one contributing an excitatory response, the other an inhibitory one), is approximated by

$$m_2(t) = 2c(y_{E,1} - y_{I,1}) + c^2(y_{E,2} - y_{I,2}) \tag{7}$$

where $y_{E,j} (j = 1, 2)$ is the jth response component of the excitatory EMD, and $y_{I,j}$ is the jth response component of the inhibitory EMD.

Let $Mr = \overline{m_2(t)}$ denote the time-averaged, or mean steady-state, response of a SIMD caused by second-order nonlinearities. Then it can easily be shown that Mr due to the moving sine-wave grating in Eq. (6) is given by

$$Mr = \frac{akc^2 L_0^2 f'(x_0)(\alpha - b)\omega}{\alpha(b^2 + \omega^2)(\alpha^2 + \omega^2)} \sin(2\pi\mu f_s \Delta s) \tag{8}$$

where $\omega = 2\pi f_t$ is the angular frequency and Δs is the interreceptor angle. From Eq. (8), we see that the SIMD mean steady-state response depends on contrast frequency $f_t = \omega/2\pi$, spatial frequency f_s, mean luminance L_0, and contrast c of the moving grating. Note that Mr is insensitive to contrast reversal (it depends on c^2) and is fully directional (i.e., its sign depends on the direction of grating motion μ).

Dependence on Contrast Frequency

The SIMD is a contrast frequency detector, not a velocity detector. The dependence of the mean-steady state response Mr on the contrast frequency, f_t, and angular velocity, f_t/f_s, is depicted in Figs. 3(a) and 3(b), respectively. The curves were obtained from Eq. (8) with parameters $a = b = 15$ and $k = 5$ and a linear activation function $f(v) = v$. The mean steady-state response increases with contrast frequency, or speed, until it reaches a maximum, and then falls off at higher fre-

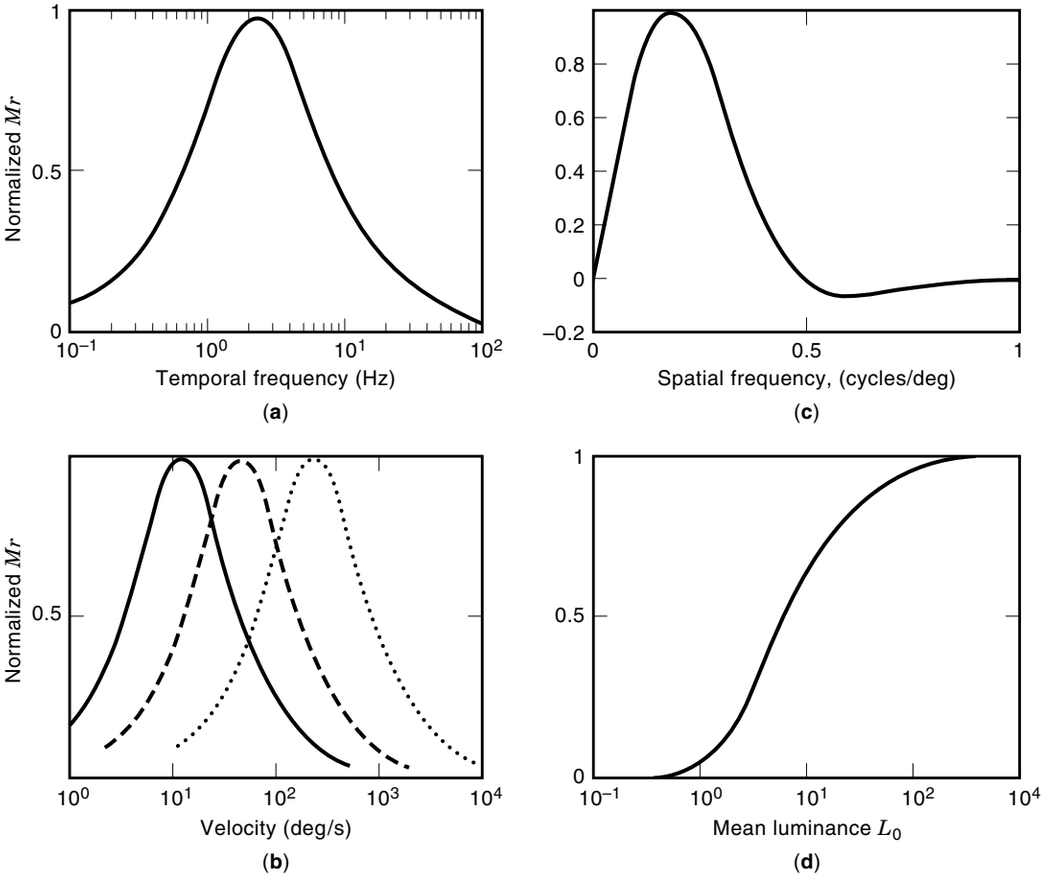

Figure 3. Mean steady-state response computed from Eq. (8) as a function of contrast frequency (a), velocity (b), spatial frequency (c), and mean luminance (d). The curves in (b) are obtained (after being normalized) for three different spatial frequencies: $f_s = 0.2$ (solid), $f_s = 0.05$ (dashed), and $f_s = 0.01$ (dotted). The curve in (c) was obtained by including the effect of contrast attenuation at the receptor level, Eq. (10).

quencies. The peak contrast frequency, the frequency of maximum steady-state response, is given by

$$f_t = \left[\frac{-(b^2+\alpha^2) + \sqrt{(b^2+\alpha^2)^2 + 12b^2\alpha^2}}{24\pi^2} \right]^{1/2} \quad (9)$$

which may be approximated by $f_t \approx b/2\pi$ at high mean luminance levels. From Eq. (8), it is evident that the peak contrast frequency does not change with spatial wavelength. However, the optimum velocity to which the system is tuned does change with the spatial frequency (Fig. 3b). The curves in Figs. 3(a) and 3(b) demonstrate the SIMD ability to respond to a broad range of pattern velocities. The response characteristics in these curves are in full agreement with those of tangential cells in the lobula plate. All DSMD neurons of the lobula plate tested so far exhibit similar response characteristics: The response does not depend on pattern velocity, but rather on contrast frequency; the response range covers about 3 log units of contrast frequency (0.01–0.05 Hz to 20–50 Hz); the response amplitudes increase from lower threshold to peak and fall off sharply above the peak; the response peaks are consistently found at 1 Hz to 5 Hz [see, e.g., Eckert (18) and Zaagman et al. (19)].

Dependence on Spatial Frequency

Equation (8) predicts a sinusoidal mean steady-state response with respect to the spatial frequency of a moving grating. Since the period of this sinusoid, with respect to spatial frequency f_s, is equal to $1/\Delta s$ (cycles/degree), responses in the range $(1/2\ \Delta s) < f_s < (1/\Delta s)$ are equal and opposite in sign to responses in the range $f_s < (1/2\ \Delta s)$. This is due to the limitations on spatial resolution set by the sampling theorem. That is, the SIMD can best resolve a grating whose spatial wavelength λ is at least twice as long as Δs the distance separating the two sampling channels (i.e., $2\ \Delta s < \lambda$). For a spatial wavelength λ such that, $\Delta s < \lambda < 2\ \Delta s$, the sign of $\sin(2\pi\mu f_s \Delta s)$ becomes opposite that of μ. Direction selectivity then reverses sign and the detector signals the wrong direction of motion. This phenomenon, known as *spatial aliasing,* is well known for insect visual systems. Eckert (18) found, by extracellular recordings from the H1 neuron, that when the spatial wavelength of the moving pattern is smaller than twice the interommatidial angle, the response properties with regard to the direction of pattern movement are reversed: Regressive motion causes inhibition and progressive motion causes excitation. However, when Buchner (20) measured behavioral responses of flies, they were not completely periodic; the negative responses measured for $\Delta\phi < \lambda < 2\Delta\phi$, where $\Delta\phi$ represents the effective interommatidial angle, were smaller in magnitude than the positive responses measured for $\lambda < 2\Delta\phi$.

So far we have always assumed that the receptors have a needle-shaped spatial sensitivity distribution (i.e., each receptor samples the visual field at a single point). However, real photoreceptors have instead an approximately Gaussian (bell-shaped) spatial or angular sensitivity distribution. They get their input by spatially integrating the luminance distribution located within their range and hence act as a spatial low-pass filter. The cutoff frequency of the low-pass filter is determined by the width of the spatial distribution at half maximum or the *acceptance angle,* $\Delta\rho$. If a sine-wave grating is presented to the photoreceptors, its contrast, c, is attenuated by a factor

$$\frac{c_r}{c} = e^{-\frac{\pi^2}{4\ln 2}(\Delta\rho/\lambda)^2} = e^{-3.56(\Delta\rho f_s)^2} \quad (10)$$

where c_r is the effective contrast in the receptors (see p. 89 in Ref. 20). Since low-pass filtering severely limits the transfer of high frequencies, we can expect the response to lose its periodicity with respect to spatial frequency. The effect of contrast attenuation on the SIMD mean steady-state response is presented in Fig. 3(c). The curve in this figure has been plotted using a contrast transfer parameter $\Delta\rho = 1$. This response resembles behavioral responses obtained from flies by Buchner (see Ref. 20 or pp. 561–621 in Ref. 14).

Dependence on Mean Luminance

In addition to the dependence on spatial and temporal frequencies, the SIMD mean steady-state response Mr depends strongly on the mean luminance of the moving pattern. Figure 3(d) depicts Mr as a function of mean luminance L_0. The variations of the curve in this figure agree well with those of the H1 neuron response. They are characterized by slow increase at low levels, saturation at high levels, and a rapid increase spanning about 2 log units of mean luminance at intermediate levels. The range of the response of H1 does also cover about 2 log units of mean luminance from threshold to saturation [see Eckert (18) and pp. 523–559 in Ref. 14]. This is different from the saturation at the photoreceptor level, which spans a range of 5 log units of mean luminance. However, since the saturation phenomenon may occur at all levels of the complex architecture of the fly visual system, we cannot know for sure if the saturation of the DSMD neurons with respect to mean luminance is caused by saturation of EMDs feeding them, as suggested here.

Adaptation of Contrast Sensitivity Function

In spatial vision, sine-wave gratings are frequently used to describe the perceptual spatiotemporal frequency response, which is commonly known as the *contrast sensitivity function* (CSF). The CSFs of visual systems are obtained by determining the inverse of the threshold contrast (i.e., the contrast sensitivity) at a set of points in the spatial frequency domain. Dvorak et al. (21) have measured at different mean luminance levels the spatial CSF for the H1 DSMD neuron in the fly lobula plate. They found that the form of the CSF varies markedly with mean luminance; in particular, the CSF increases as the mean luminance level of the stimulus is raised. At high mean luminance levels, the CSF peaks at a certain spatial frequency and falls off at higher and lower frequencies. Moreover, the high frequency roll-off becomes less steep and the peak frequency shifts toward lower frequencies as mean luminance decreases.

The adaptation, or change, of CSF upon change of mean luminance level can be accounted for by considering the response of a SIMD to a moving sinusoidal grating and the light adaptation phenomena that occur at the photoreceptor level. Equation (8), with $a = b = 15$ and $k = 10$, was used to compute normalized CSFs at different values of L_0. The CSF curves in Fig. 4 were obtained by including the effect of spatial filtering that takes place at the receptor level—that is, by

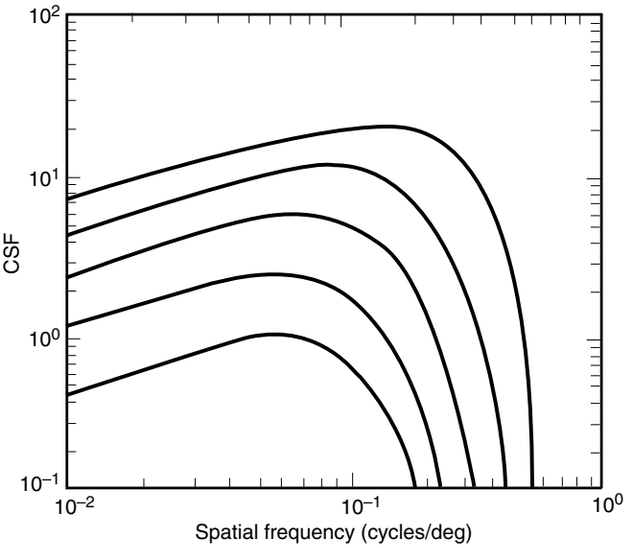

Figure 4. CSF of a SIMD as computed from Eq. (8) for different mean luminance levels: $L_0 = 5$, 2, 1, 0.5, and 0.25 (from top to bottom).

multiplying the contrast with the term $e^{-3.56(\Delta\rho_s^\circ)^2}$. Figure 4 clearly demonstrates that the CSF of the SIMD adapts to mean luminance changes in the same way the CSF of DSMD (the H1 unit) neuron does. Using an effective contrast transfer parameter (the acceptance angle) $\Delta\rho$ that depends on mean luminance results in pushing the peak frequency of the CSF to a lower value. It is well known that in insect compound eyes the effective contrast transfer parameter, $\Delta\rho$, increases upon lowering the mean luminance level L_0. This increase of $\Delta\rho$ is due to a mechanism of adaptation to low light

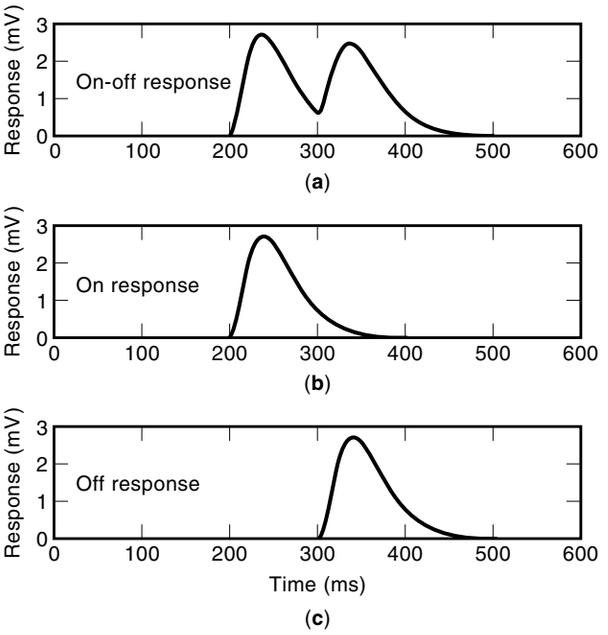

Figure 5. Response of the neural network model (Fig. 1) to stimulation of a pair of adjacent receptors with a sequence of flashes mimicking motion in the preferred direction. (a) ON-OFF response: The first flash is turned on at $t = 100$ ms and turned off at $t = 200$ ms followed by the second flash, which is turned on at $t = 200$ ms and turned off at $t = 300$ ms. (b) ON response: The onset of the first flash ($t = 100$ ms) is followed by the onset of the second flash ($t = 200$ ms), and both flashes are turned off at $t = 300$ ms. (c) OFF response: Both flashes are turned on at $t = 0$ ms, but the first flash is turned off at $t = 100$ ms and the second is turned off at $t = 200$ ms.

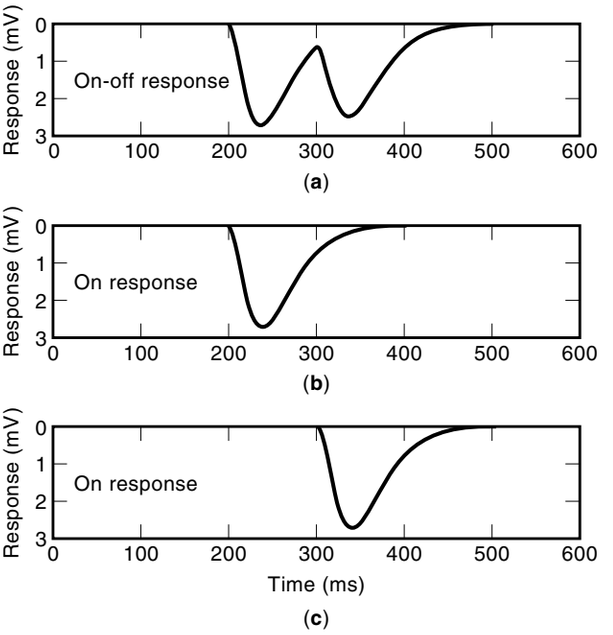

Figure 6. Response of the neural network model (Fig. 1) to stimulation of a pair of adjacent receptors with a sequence of flashes mimicking motion in the null direction. (a) ON-OFF response: The first flash is turned on at $t = 100$ ms and turned off at $t = 200$ ms followed by the second flash, which is turned on at $t = 200$ ms and turned off at $t = 300$ ms. (b) ON response: The onset of the first flash ($t = 100$ ms) is followed by the onset of the second flash ($t = 200$ ms); both flashes are turned off at $t = 300$ ms. (c) OFF response: Both flashes are turned on at $t = 0$ ms, but the first flash is turned off at $t = 100$ ms and the second is turned off at $t = 200$ ms.

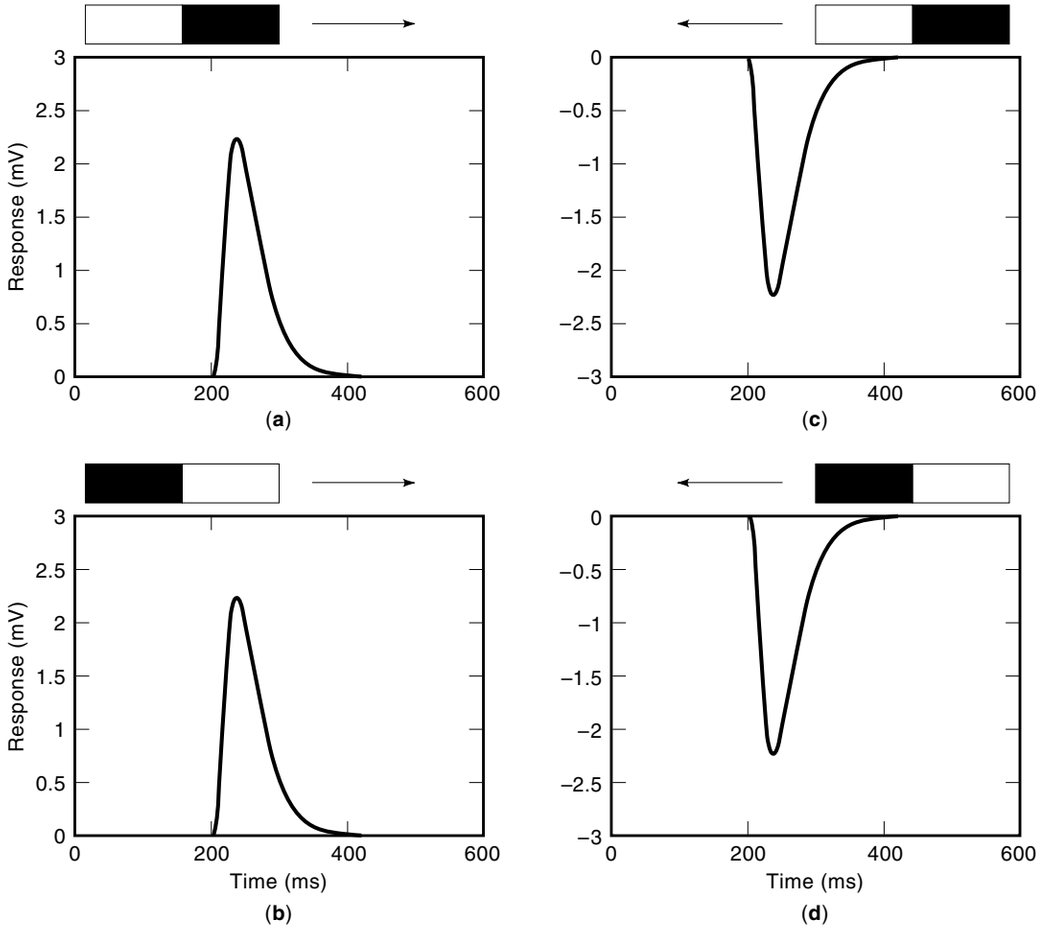

Figure 7. Response of the neural network to a jumping edge. At $t = 0$ the edge, whose orientation (black-white or white-black) is indicated above the plot, appears over the pair of adjacent receptors. After 200 ms, it jumps by one receptor to the right, (a) and (b), or to the left, (c) and (d).

levels that results in widening the angle subtended by the photoreceptive waveguides, hence increasing absolute sensitivity by sacrificing spatial acuity (for more details on adaptational mechanisms in compound eyes, see, e.g., pp. 30–73 in Ref. 13 and pp. 391–421 in Ref. 10).

Response to Sequential Flashes and Jumps

In this subsection simulation results are presented that show that a DSMD architecture (Fig. 1) based on the SIMD can account for the recorded responses of the H1 neuron to a variety of moving stimuli. In the simulations, the input signal is passed through a log transformation, representing the transformation at the photoreceptor level. A laminar unit (L-Unit, Fig. 1) is simulated as a highpass filter (see, e.g., pp. 213–234 in Ref. 13). After the signal is magnified, it is rectified to produce transient responses of ON and OFF nature; there is strong evidence that, in the insect visual system, the motion signals are carried through separate ON and OFF channels [see pp. 360–390 in Ref. 13 and also Horridge and Marcelja (22)]. The outputs of the ON and OFF channels are then lowpass filtered and passed laterally to interact, respectively, with the outputs of the ON and OFF channels in the adjacent columns. Here, the interaction used at the EMD level is a SIMD, Eq. (2), with parameter values $a = 50$, $\tau = 40$ m, and $k = 20$.

The spatial integration of local movement signals at the level of the wide-field DSMD neurons is, in principle, almost linear if the activation of single input channels produce only minute voltage changes at the output sites of the dendrites. If we assume it to be linear, then the effects of the excitatory and inhibitory synaptic contacts of the individual EMDs with the DSMD neurons are, respectively, additive and subtractive. Thus, if we denote by $m_{Ej}(t)$ the signal mediated by the jth excitatory synapse and by $m_{Ij}(t)$ the signal mediated by the jth inhibitory synapse, then, to first order, the response of the DSMD neuron is given by

$$R(t) = \sum_j m_{Ej}(t) - m_{Ij}(t) \tag{11}$$

where the summation operation is carried over all j indices for both ON and OFF channels, and the rates of change of $m_{Ej}(t)$ and $m_{Ij}(t)$ are given by Eq. (2). Here the response $R(t)$ represents the actual membrane voltage, or deviation of the

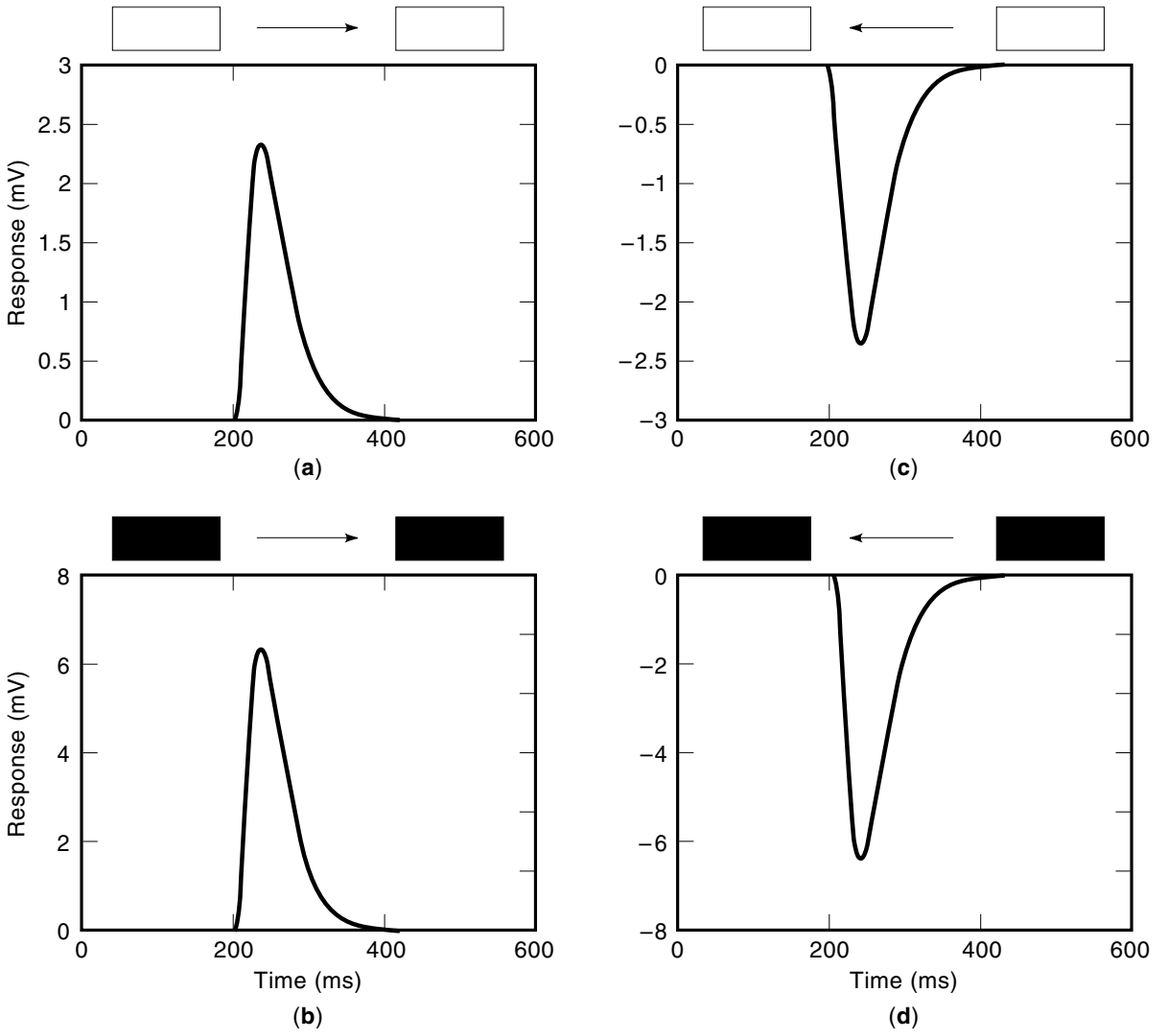

Figure 8. Response of the neural network to a jumping thin bar. At t = 150 ms, a bright or dark bar appears over one receptor and disappears at t = 175 ms. Then at t = 200 ms, the same bar reappears over a neighboring receptor to the right (a) and (b), or to the left (c) and (d). The responses are directional regardless of bar contrast.

membrane voltage from the resting potential, rather than the firing rate of the neuron. To obtain the response as firing rate, the output of the DSMD neuron should be passed through a rectifying nonlinearity.

Response to Sequential Flashing. Simulations of the neural network responses to light flashes showed that stimulating a pair of receptors singly or synchronously does not evoke any response in the DSMD neuron (results not shown). However, stimulating the two receptors with a sequence mimicking motion in the preferred direction induces an excitatory response (Fig. 5). Note that the response of the network is always time locked to the onset or offset of the second flash. Note also that the response to a sequence of nonoverlapping light flashes, with a short time lag between their onsets, consists of two prominent peaks [Fig. 5(a)]; the first peak is caused by the onset sequence [Fig. 5(b)] and the second one by the offset sequence [Fig. 5(c)]. The responses of the network to sequences mimicking motion in the null direction are shown in Fig. 6. These responses are equal but of opposite polarity to those shown in Fig. 5; they are inhibitory responses. The responses in Figs. 5 and 6 are similar to those recorded by Franceschini and his colleagues from the H1 neuron (pp. 360–390 in Ref. 13).

Response to Jumps. The responses of the neural network to an object (an edge or a bar) jumping over a distance equal to the distance between neighboring receptors are presented in Figs. 7 and 8. Figure 7 shows that, regardless of its orientation, an edge jumping in the preferred direction induces excitation [Figs. 7(a) and 7(b)], while an edge jumping in the null direction causes inhibition of the DSMD-neuron [Figs. 7(c) and 7(d)]. The dependence of directionality upon contrast was tested by jumping a thin light or dark bar in the preferred and null directions. The results are presented in Fig. 8, which shows that the preferred direction of the neural network model does not depend on the sign of contrast. In other words, both a bright and a dark bar evoke an excitatory response

when jumping in the preferred direction [Figs. 8(a) and 8(b)], and an inhibitory response when jumping in the null direction [Figs. 8(c) and 8(d)]. Notice, though, that the dark bar elicits a stronger response than the bright bar does. This phenomenon has also been observed in the recorded responses of the H1 neuron of *Calliphora stygia* by Horridge and Marcelja (22), who also found that the directionality of the H1 neuron does not change with edge orientation or bar contrast (Figs. 2 and 5 in Ref. 22). However, they found that the H1 neuron may lose its directionality by reversing the contrast of the jumping bar. More specifically, when there is a time lag during the jump the H1 neuron preserves its directionality (Fig. 5 in Ref. 22, but when there is no time lag (i.e., the second bar appears—contrast reversed—simultaneously with the disappearance of the first one), the H1 neuron seems to lose its directionality (Fig. 6 in Ref. 22).

The responses of our neural network model to bars that reverse contrast at the jump are depicted in Figs. 9 and 10. Despite contrast reversal, the network preserves its directionality when there is a time lag between the disappearance and reappearance of the bar (Fig. 9). Yet the network may lose its directionality if there is no time lag during the jump (Fig. 10). Although the onset of the dark bar followed by the offset of the light bar constitutes a preferred OFF sequence in Fig. 10(b), the response is inhibitory. The reason for reversal of directionality in Figs. 10(b) and 10(d) is that the sequence caused by the onset and offset of the black and white bars, respectively, evokes only a weak excitatory [Fig. 10(b)] or inhibitory [Fig. 10(d)] response in the DSMD neuron, for the time lag of the sequence is too long (150 ms). This weak response is dominated by an opposite ON response induced by the simultaneous appearance and disappearance of the white and black bars, respectively. Since the ON response caused by the offset of the black bar is not exactly the same as the ON response caused by the onset of the white bar, there is an imbalance between the excitatory and inhibitory signals fed to the DSMD neuron—two adjacent EMDs are inhibited simultaneously, but their two immediate neighbours are not—which gives rise to an excitatory or inhibitory ON response. The opposite happens when reversing the contrast of the bars [Fig. 10(c)].

ELECTRONIC ANALOGS OF CYBERNETIC MODELS

Since cybernetics is the parallel study of living organisms and machines, these parallels can both inspire and guide develop-

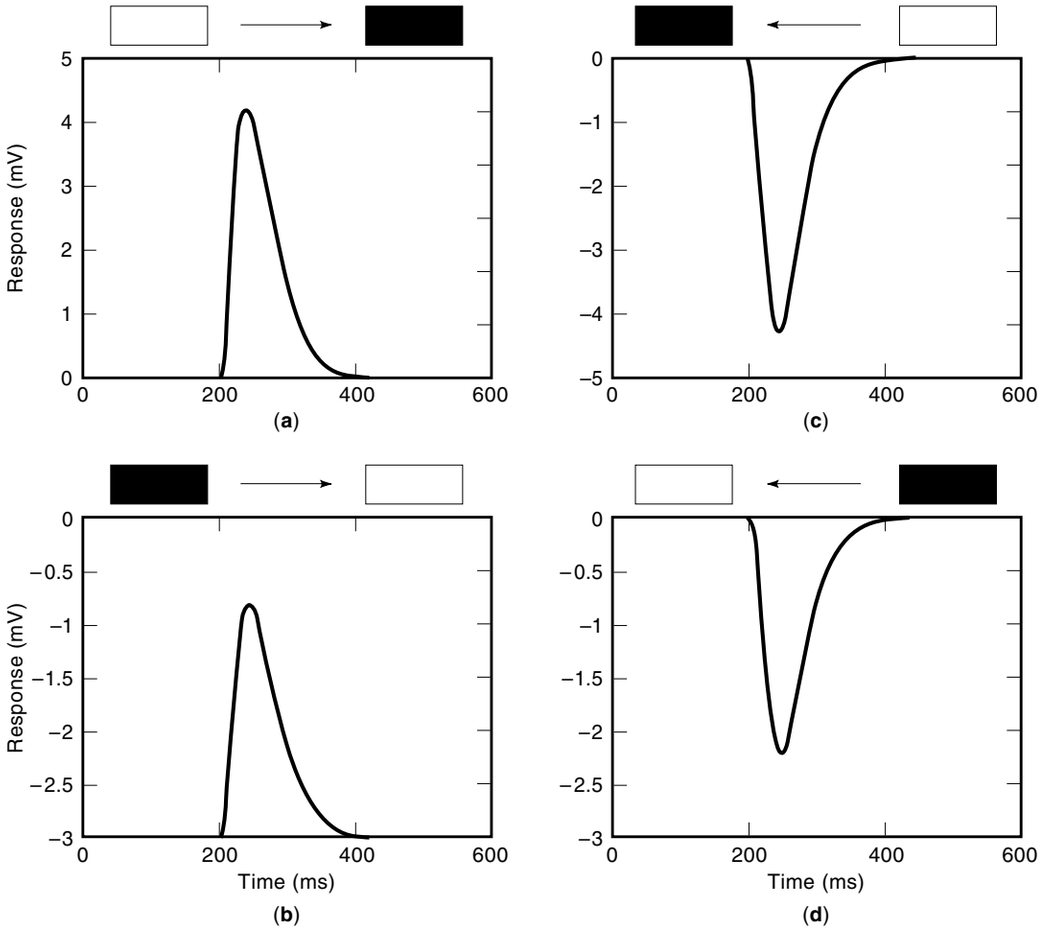

Figure 9. Response of the neural network model to contrast reversal. The stimulus conditions are the same as those of (Fig. 8), except for reversal of contrast at the jump (i.e., a black bar becomes white and vice versa). The responses are directional in spite of contrast reversal.

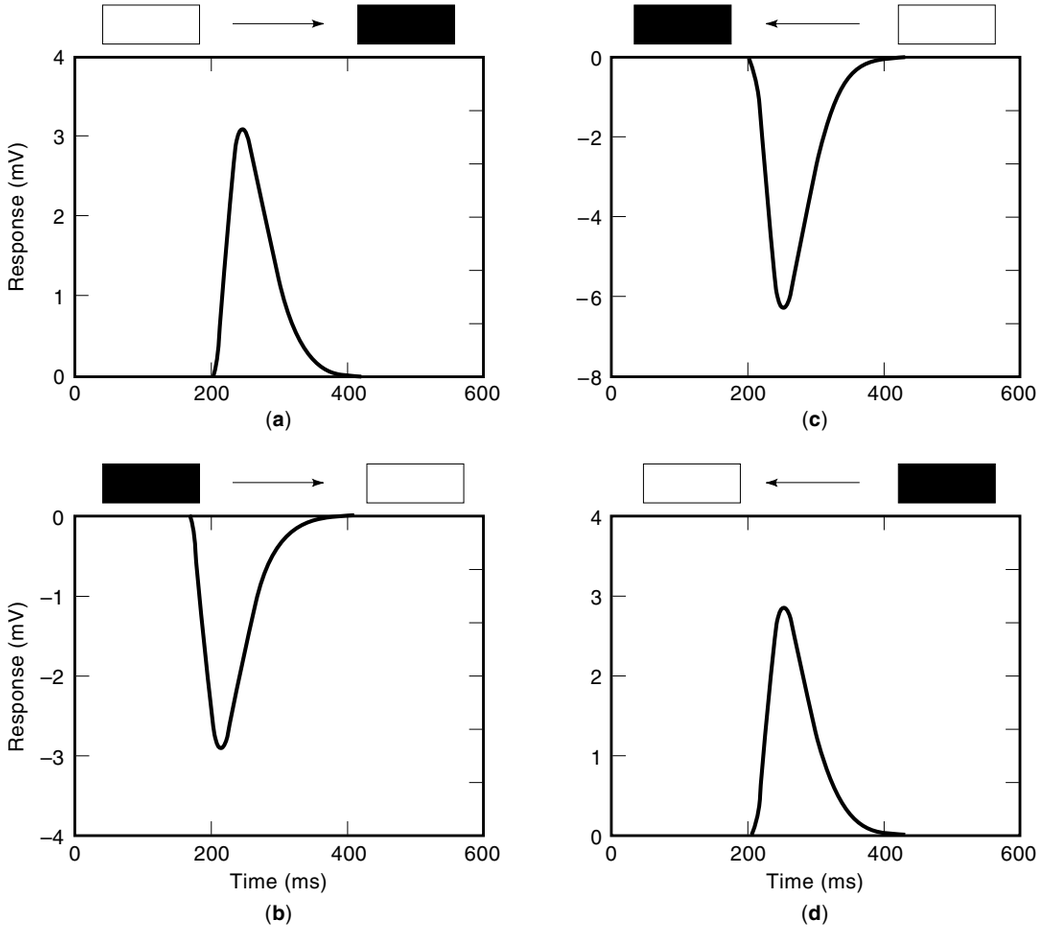

Figure 10. Response of the neural network to contrast reversal. At $t = 50$ ms, a bar appears over one receptor. Then, at $t = 200$ ms, the bar reappears, with its contrast reversed, over a neighboring receptor. Here, a jump in the preferred direction can cause a negative response (b), and a jump in the null direction can cause a positive response (d).

ment of the latter based on the former. Nerve cells' conductance variation leads to simple analog electronic circuits that possess rich signal processing capabilities. Similar to the developments of the previous section, simple components are combined to demonstrate increasingly more complicated processing, such as motion detection. Parallelism, fault tolerance, simplicity of each processing unit, and repeatability of the circuits make hardware implementation of the nerve cell models feasible. One important aim of such implementations is to integrate sensing and processing units on the same substrate, thus increasing the speed of operation and reducing bandwidth necessary to transmit the sensed information to higher levels of processing, much as the retina performs this function for higher processing in the cerebral cortex. The communications bottleneck is avoided by performing much of the signal processing in the sensor itself. Networks of the kind described by Eq. (1) contain multiplicative terms, which arise from the control of conductance in nerve membrane (23). It is natural to utilize control of shunting paths of current in electronic implementations, such as the field-effect transistor (FET) and complementary metal-oxide semiconductor (CMOS) devices, in their "triode" or sub-pinch-off regions. If the gate voltages are received from the outputs of other network devices, a network of feedforward (literally as written in Eq. 1) interconnection is synthesized. If the other network devices, in turn, receive their gate voltages from the outputs of the first set, a feedback interconnection occurs. In general, the design is more direct using the feedforward strategy, but of course the feedback strategy carries with it certain robustness, insensitivity to parameter change, and fault tolerance. It is further a point that biological nerve networks may also be feedback or feedforward. In many experimental studies the determination of which alternative is actually "wired" is a goal, but there is no clear dominance of one strategy, nor evidence for optimization based on cost functions in the short term. Perhaps more important than these considerations are the nonlinearities of the networks. These are primarily the multiplicative terms such as those in Eq. (1). These accomplish fractional power automatic gain control, an approximation to the Weber–Fechner law originally established in psychophysics of human observers and shown to be in the visual system primarily due to automatic gain control by the photoreceptors (23). The multiplicative terms in electronic implementations clearly optimize the use of the limited dynamic range of devices in comparison with linear implementations (Fig. 6, p. 469 in Ref. 10). But further important adaptation

mediated by these multiplicative terms is found in the temporal and spatial contrast enhancement and "tuning," which changes with mean light level in a systematic and near-optimal manner (23). This is related to the relatively higher amplification of higher temporal and spatial frequencies by the visual systems at higher light levels (as seen in the adaptation of the CSF in Fig. 4), where more photons are available to be processed and not simply counted (23). In the early work of David Marr on early vision, an underlying center-inhibitory surround spatial impulse response was invoked (24). However, these biological, mathematical, and electronic analyses show that such spatial and temporal impulse responses must adapt and change their configuration to become more differentiating in brighter light (25,26). This is simply a strategy to make use of the available optical information in order to see better (27,28).

BIBLIOGRAPHY

1. N. Wiener, *Cybernetics,* 2nd ed., Cambridge, MA: MIT Press, 1961.
2. N. Wiener, *The Human Use of Human Beings: Cybernetics and Society,* rev. ed., Garden City, NY: Doubleday, 1954.
3. S. J. Heims, *The Cybernetics Group,* Cambridge, MA: MIT Press, 1991.
4. W. H. Calvin, *The Cerebral Code,* Cambridge, MA: MIT Press, 1996.
5. W. J. Rugh, *Nonlinear System Theory: The Volterra / Wiener Approach,* Baltimore: Johns Hopkins University Press, 1981.
6. P. Z. Marmarelis and V. Z. Marmarelis, *Analysis of Physiological Systems,* New York: Plenum, 1978.
7. M. Schetzen, *The Volterra and Wiener Theories of Nonlinear Systems,* Malabar: Krieger, 1989.
8. H.-W. Chen et al., Nonlinear analysis of biological systems using short M-sequences and sparse-stimulation techniques, *Ann. Biomed. Eng.,* **24**: 513–536, 1996.
9. M. J. Korenberg and I. W. Hunter, The identification of nonlinear biological systems: Volterra kernel approaches, *Ann. Biomed. Eng.,* **24**: 250–268, 1996 [and reprised in **24** (4)].
10. R. B. Pinter and B. Nabet (eds.), *Nonlinear Vision: Determination of Neural Receptive Fields, Function, and Networks,* Boca Raton, FL: CRC Press, 1992.
11. W. Reichardt, T. Poggio, and K. Hausen, Figure-ground discrimination by relative movement in the visual system of the fly, Part II: Towards the neural circuitry, *Biolog. Cybernetics,* **46** (Suppl): 1–30, 1983.
12. N. J. Strausfeld, *Atlas of an Insect Brain,* New York: Springer-Verlag, 1976.
13. D. G. Stavenga and R. C. Hardie (eds.), *Facets of Vision,* Berlin: Springer-Verlag, 1989.
14. M. A. Ali (ed.), *Photoreception and Vision in Invertebrates,* New York: Plenum, 1984.
15. K. Kirschfeld, The Visual System of Musca: Studies on Optics, Structure and Fusion, in R. Wehner (ed.), *Information Processing in the Visual Systems of Arthropods,* New York: Springer-Verlag, 1972, pp. 61–74.
16. H. B. Barlow and W. R. Levick, The mechanism of directionally selective units in the rabbit's retina, *J. Physiol.,* **178**: 477–504, 1965.
17. A. Bouzerdoum, The elementary movement detection mechanism in insect vision, *Proc. R. Soc. Lond.,* **B339**: 375–384, 1993.
18. H. Eckert, Functional properties of the H1-neurone in the third optic ganglion of the blowfly, *Phaenicia, J. Comp. Physiol.,* **A-135**: 29–39, 1980.
19. W. H. Zaagman, H. A. K. Mastebroek, and J. W. Kuiper, On the correlation model: performance of a movement detecting neural element in the fly visual system, *Biol. Cybern.,* **31**: 163–168, 1978.
20. E. Buchner, Elementary movement detectors in an insect visual system, *Biol. Cybern.,* **24**: 85–101, 1976.
21. D. Dvorak, M. V. Srinivasan, and A. S. French, The contrast sensitivity of fly movement-detection neurons, *Vision Res.,* **20**: 397–407, 1980.
22. G. A. Horridge and L. Marcelja, Responses of the H1 neuron of the fly to jumped edges, *Phil. Trans. R. Soc. Lond.,* **B-329**: 65–73, 1990.
23. B. Nabet and R. B. Pinter, *Sensory Neural Networks: Lateral Inhibition,* Boca Raton, FL: CRC Press, 1991.
24. D. C. Marr, *Vision: A Computational Investigation into the Human Representation and Processing of Visual Information,* San Francisco: W. H. Freeman, 1982.
25. M. V. Srinivasan, S. B. Laughlin, and A. Dubs, Predictive coding: a fresh view of inhibition in the retina, *Proc. R. Soc. Lond.,* **B-216**: 427–459, 1982.
26. M. V. Srinivasan, R. B. Pinter, and D. Osorio , Matched filtering in the visual system of the fly: Large monopolar cells of the lamina are optimized to detect moving edges and blobs, *Proc. R. Soc. Lond.,* **B-240**: 279–293, 1990.
27. J. J. Atick and A. N. Redlich, What does the retina know about natural scenes?, *Neural Computation,* **4**: 196–210, 1992.
28. J. H. van Hateran, Theoretical predictions of spatio-temporal receptive fields of fly LMCs, and experimental validation, *J. Comp. Physiol.,* **A-171**: 157–170, 1992.

ROBERT B. PINTER
University of Washington

ABDESSELEM BOUZERDOUM
Edith Cowan University

BAHRAM NABET
Drexel University

CYCLIC CONTROL. See PERIODIC CONTROL.

CYCLOCONVERTERS. See AC-AC POWER CONVERTERS.

CYCLOTRONS. See SUPERCONDUCTING CYCLOTRONS AND COMPACT SYNCHROTRON LIGHT SOURCES.